Journal of Power Sources 195 (2010) 3794–3801

Contents lists available at ScienceDirect

Journal of Power Sources

journal homepage: www.elsevier.com/locate/jpowsour

Solvent-assisted graphite loading for highly conductive phenolic resin bipolar plates for proton exchange membrane fuel cells

Soo-Jung Kang[a], Dong Ouk Kim[a], Jun-Ho Lee[a], Pyoung-Chan Lee[a], Min-Hye Lee[a], Youngkwan Lee[b], Jun Young Lee[b], Hyouk Ryeol Choi[c], Jong-Ho Lee[d], Yong-Soo Oh[e], Jae-Do Nam[a,f,*]

[a] Department of Polymer Science and Engineering, Sungkyunkwan University, Republic of Korea
[b] Department of Chemical Engineering, Sungkyunkwan University, Republic of Korea
[c] School of Mechanical Engineering, Sungkyunkwan University, Suwon 440-746, Republic of Korea
[d] LS Industrial Systems, Ltd., Anyang 431-831, Republic of Korea
[e] Samsung Electro-Mechanics, Co. Ltd., Suwon, Republic of Korea
[f] Department of Energy (WCU), Sungkyunkwan University, Republic of Korea

ARTICLE INFO

Article history:
Received 17 June 2009
Received in revised form 5 October 2009
Accepted 9 November 2009
Available online 20 November 2009

Keywords:
Proton exchange membrane fuel cell
Bipolar plate
Conductivity
Solvent-assisted graphite
Phenolic resin

ABSTRACT

A highly conductive polymer-based bipolar plate is fabricated using phenolic resin and graphite for proton exchange membrane fuel cells (PEMFCs). In order to load graphite fillers up to 90 wt% and minimize the void volume, the wetting properties of the graphite and phenolic resin are key factors for ensuring high electrical conductivity of the bipolar plates through good contact and uniform dispersion of graphite fillers. Since the surface free-energies of the phenolic resin and graphite are significantly different at 107.77 and 43.3 mJ m^{-2}, respectively, to give a high contact angle of 87.1°, methanol with 19.6 mJ m^{-2} of surface energy is incorporated to decrease the contact angle between the matrix and graphite to 11.2°. By adjusting the surface energy of the matrix system, the conductivity of a composite containing 90 wt% of graphite reaches 379 S cm^{-1}. The air permeability of the composite containing 80 wt% of graphite is less than 5×10^{-6} cm^3 cm^{-2} s without open pores. The flexural modulus ranges from 6700 to 11000 MPa for graphite loads between 60 and 80 wt%, respectively.

1. Introduction

Bipolar plates are major components of a proton exchange membrane fuel cell (PEMFC) stack and account for almost 80% of the total weight and 50% of the total cost [1,2]. The bipolar plates must have high electrical conductivity, sufficient mechanical integrity, good corrosion resistance, low gas permeability and low-cost, if they are to be widely used [3].

Several types of material are used for the bipolar plates, e.g., metal plates, polymer-coated metal plates, graphites, carbon–carbon composites and graphite–polymer composites [4]. Metallic bipolar plates usually have high bulk electrical and thermal conductivities, good mechanical properties, negligible gas permeability, and are amenable to mass production. Since metal bipolar plates have low corrosion resistance, however, a conductive and low-cost coating must be applied to the surfaces of the plates to form a protective layer. This process is still considered difficult to accomplish [5]. In addition, metal plates are heavy and hence disadvantageous in transportation applications.

The most commonly used bipolar plate is made from graphite. Graphite bipolar plates have good electrical conductivity, excellent corrosion resistance, and low density. The problems with such plates are brittleness and the porous structure, along with the extra-cost associated with machining the gas flow channels into the plates [6]. More importantly, due to the porous nature of graphite, post-processing (such as resin impregnation) is usually required to render the bipolar plate impermeable to fuel and gases [7].

An alternative to graphite or metal bipolar plates is a graphite-based composite bipolar plate, which consists of graphite fillers and polymer resin and is fabricated via conventional polymer processing methods. Composite bipolar plates have been the subject of intense study with the focus on their electrical conductivity and mechanical properties [6,8–12]. At present, phenolic resin is considered to be one of the more desirable matrix candidates, due to its well-balanced thermal stability and mechanical properties under the harsh electrochemical conditions of fuel cell utilization.

Phenolic resin has a high char yield with excellent thermal resistance properties [13]. In the bipolar plate fabrication process, the polymer not only acts as a binder, but also influences the performance of the bipolar plate. Properties such as electrical

* Corresponding author at: Department of Polymer Science and Engineering, Sungkyunkwan University, 300 Chunchun-Dong, Jangan-Ku, Suwon 440-746, Kyunggi-Do, Republic of Korea. Tel.: +82 31 299 4062; fax: +82 31 299 4069.
E-mail address: jdnam@skku.edu (J.-D. Nam).

0378-7753/$ – see front matter © 2009 Elsevier B.V. All rights reserved.
doi:10.1016/j.jpowsour.2009.11.064

conductivity, flexural strength, shore hardness and porosity are all affected by the properties of the polymer in the bipolar plate. Polymeric matrix precursors having polar atomic groups or single or pairs of single electrons in their molecular configuration are easy to polarize or delocalize, thereby allowing electrical channels to be easily formed. In this sense, the polar atomic groups in the phenolic resin (such as –OH groups and double bonds) are beneficial for improving plate conductivity and thereby causing the resin to be an excellent polymer matrix for bipolar plates [14].

For graphite–polymer composite bipolar plates, the injection moulding process has been adopted using polypropylene as a binder [15–17]. Unfortunately, however, the melt viscosity of thermoplastic polymers is so high that the graphite loading is physically limited, especially for large and thin bipolar plates. A wet-lay process using poly(vinylidene fluoride) has been adopted for highly loaded graphite bipolar plates, but the manufacturing productivity of this method needs improving [18]. With respect to bipolar plate manufacturing processes, it should be mentioned that a good wetting characteristic between the filler and the polymer is crucial in the case of highly loaded composite systems. When the filler content is high, the mixture viscosity becomes very high and thus bad wetting characteristics promote void formation at the filler|matrix interface, which substantially decreases electrical conductivity and degrades the mechanical properties to give an increased gas permeability.

Accordingly, we investigated the wetting properties of the graphite and phenolic resin, and improved the wetting characteristics of these two phases by incorporating an appropriate solvent to decrease the contact angle between the graphite and resin system. By examining the electrical conductivity, mechanical properties, gas permeability and composite morphology, it is found that the interfacial energy is the critical factor to ensure a highly loaded conductive composite system.

2. Experimental

2.1. Materials

The thermosetting resin used in this study was a resole-type phenol resin (Kangnam Chemical Co. Ltd., Korea). Graphite powders having average particle sizes of 75 μm (GR75) and 150 μm (GR150) were obtained from Timcal Co. Ltd., Switzerland. Methanol, ethylene glycol and formamide were purchased from Sigma–Aldrich Corporation.

2.2. Preparation of composite bipolar plates

Phenolic resin and methanol were mechanically stirred at a weight ratio of 50:50 for 5 min at room temperature. The graphite loading content varied from 35 to 90 wt% of graphite. After mixing the resin, graphite powder and methanol at room temperature for 30 min using a kneader, methanol was evaporated in a vacuum oven at 30 °C for 2 h, which eliminates 99% (by weight) of the methanol. For each sample, the mixture was place in a mould (100 mm × 100 mm × 2 mm) and pre-heated in a hot press at 50 °C for 30 min. The sample was then pressed at 10.7 MPa and 80 °C for 30 min and cured at 200 °C for 60 min. Some of the composite specimens were then post-cured at 210 °C for 10 min under pressure.

2.3. Electrical conductivity of graphite powder in through-thickness direction

To determine the electrical conductivity of the graphite powder, the graphite powder and ethyl alcohol were mixed in a weight ratio of 1:1 and dispersed by ultra-sonication at room temperature for 1 h. After complete dispersion, the ethyl alcohol was evaporated in a vacuum oven at 80 °C for 48 h. The graphite powder (0.05 g) was then packed in a cylinder and then compressed with an Instron Universal Testing Machine (LR30K Plus 30 kN, LLOYD Instruments, Inc., UK), as seen in the experimental set-up in Fig. 1. While the sample was being compressed, the electrical conductivity of the graphite powder was monitored in situ as a function of the volume fraction. The scanning election microscopic images in Fig. 2 show the morphology of the graphite powders, GR75 and GR150. It can be seen that the overall particle size of GR75 (Fig. 2A and B) is smaller than those of GR150 (Fig. 2C and D). Although the average size of GR150 is larger than GR75, both of them include various sizes of graphite fragments, which would give good packing characteristics and electrical percolation in the composites.

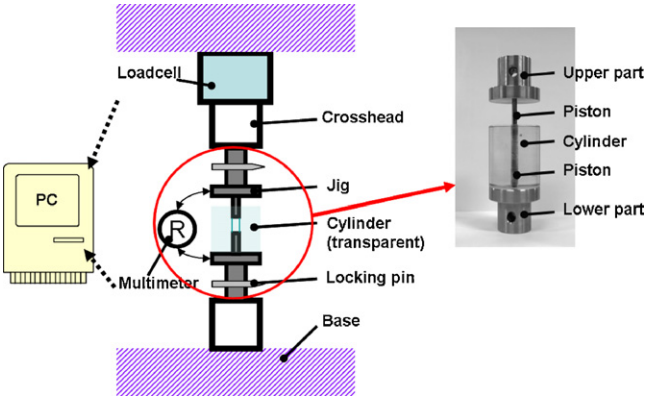

Fig. 1. Experimental set-up for measuring electrical conductivity of graphite powder as a function of graphite content.

2.4. Bipolar plate characterization

The in-plane electrical conductivities of the graphite composites (containing 60–90 wt% loading of either GR75 or GR150) were measured by a four-point probe method. Samples were cut into 100 mm × 5 mm × 2 mm pieces. Their conductivities were measured at four different positions, and the average was taken. Electrical resistance was measured using an OHM meter (Chitai 5601, Taiwan) and the electrical conductivity was calculated. Flexural strength was measured by a three-point bending method (ASTM D790), using samples with 50 mm × 25 mm × 2 mm dimensions. A universal testing machine (LR30K Plus 30 kN, LLOYD Instruments, Inc., UK) was used to test the samples. The reported values are the average flexural strength obtained from testing four samples. Gas permeability was measured by a capillary flow porometer (CFP-1200AEX, USA). The microstructure of the composite samples was studied with a scanning electron microscope (Hitachi S-2140, Japan) and an optical microscope (Olympus BX51, Japan). The contact angles of phenol resin, methanol, and a phenolic resin and methanol mixture on graphite plates (Infrazone Ltd., Korea) were measured by means of a contact angle meter (DI, GBX Instrument, France) via the sessile drop method.

3. Results and discussion

3.1. Comparison of contact angle values

Fig. 3(A) shows that the contact angle image of phenolic resin placed on the graphite plate is 87.1°. It is considered that this contact angle is too high to give a good wetting characteristic. Especially when the loading content of the graphite particle is fairly high, e.g., up to 90 wt%, such a high contact angle may very well give entrapped voids during mixing processing, that result in a poor interface between the graphite and phenolic resin.

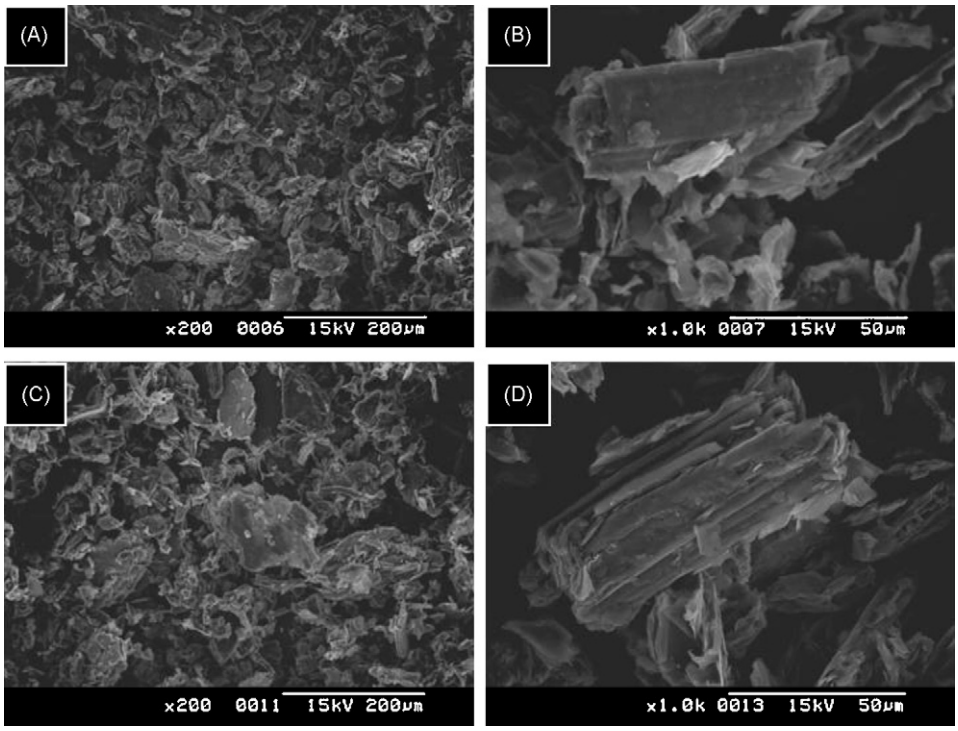

Fig. 2. SEM images of graphite powder of GR75 (A and B) and GR150 (C and D) at different magnifications.

In practice, when the loading content of the graphite is greater than ca. 40 wt%, the resin–graphite mixture usually does not provide a continuous liquid phase but a discontinuous solid phase. It should be mentioned that even a small number of entrapped voids and flaws at the interface would result in a critical deterioration in strength/stiffness, electrical conductivity and gas permeability, which are the most important properties in the fuel cell bipolar plates.

In order to enhance the wetting characteristics of phenolic resin on the graphite, measurements were made of the surface energies of the graphite plate and phenolic resin using reference materials. The surface free-energies of materials can be determined by the contact angle measurements and the following equation (Young's equation).

$$\gamma_S = \gamma_L \cos\theta + \gamma_{SL} \quad (1)$$

where: γ_S, γ_L and γ_{SL} are the surface free-energy of the solid, the surface tension of the liquid, and the interfacial energy between the solid and liquid, respectively; θ is the contact angle between the solid and the liquid. The surface free-energy of a solid or liquid may be separated into a Lifshitz–van der Waals component (γ_{LW}) and a Lewis acid–base component (γ_{AB}) as follows [19]:

$$\gamma = \gamma^{LW} + \gamma^{AB} \quad (2)$$

Furthermore, the Lewis acid–base component may be expressed as

$$\gamma^{AB} = 2(\gamma^+\gamma^-)^{1/2} \quad (3)$$

where γ^+ and γ^- represent the electron-acceptor and electron-donor parameters of γ, respectively. The interfacial energy may be calculated using the following equation [20]:

$$\gamma_{SL} = \gamma_S + \gamma_L - 2[(\gamma_S^{LW}\gamma_L^{LW})^{1/2} + (\gamma_S^+\gamma_L^-)^{1/2} + (\gamma_S^-\gamma_L^+)^{1/2}] \quad (4)$$

Coupling Eq. (4) with Eq. (1) leads to

$$\gamma_L(1+\cos\theta) = 2[(\gamma_S^{LW}\gamma_L^{LW})^{1/2} + (\gamma_S^+\gamma_L^-)^{1/2} + (\gamma_S^-\gamma_L^+)^{1/2}] \quad (5)$$

Thus, it is possible to determine the $\gamma_S{}^{LW}$, $\gamma_S{}^+$ and $\gamma_S{}^-$ components of the surface free-energy of the solid in Eq. (5) by measuring the contact angles with three liquids, whose $\gamma_L{}^{LW}$, $\gamma_L{}^+$ and $\gamma_L{}^-$ components are known, and vice versa. In this study, three reference liquids of water, ethylene glycol and formamide were used to determine the surface free-energies of solid substrate materials, namely, graphite plate, glass plate and silicon wafer in this study. Then these three substrates were used to determine the surface free-energies of phenolic resin.

The $\gamma_L{}^{LW}$, $\gamma_L{}^+$ and $\gamma_L{}^-$ of the three reference liquids are summarized in Table 1. More specifically, the measured contact angles of water, ethylene glycol and formamide on the graphite plate 65.6°, 36.8° and 47.5°, respectively. These contact angles were substituted into Eq. (5) to give three equations including three unknown components of graphite, resulting in γ_S, $\gamma_S{}^{AB}$ and $\gamma_S{}^{LW}$ values for graphite of 43.3, 5.4 and 37.9 mJ m^{-2}, respectively (see Table 1). Similarly, these three reference liquids were also used to measure the surface free-energies of the glass plate and silicon wafer in order to use them as reference solid substrate materials. As a result, the surface energies of γ_S, $\gamma_S{}^{AB}$ and $\gamma_S{}^{LW}$ are 121.61, 30.98 and 90.63 mJ m^{-2} for the glass plate and 138.95, 3.93 and 135.02 mJ m^{-2} for the silicon wafer, respectively, which are also summarized in Table 1.

Table 1
Surface free-energies (mJ m^{-2}) of reference liquids, phenolic resin and solid substrates.

	Phase	γ	γ^{AB}	γ^{LW}	γ^+	γ^-
Water[a]	Liquid	72.8	51.0	21.8	25.5	25.5
Ethylene glycol[a]	Liquid	48.0	19.0	29.0	1.92	47.0
Formamide[a]	Liquid	58.0	19.0	39.0	2.28	39.6
Phenolic resin	Liquid	107.77	51.63	56.14	11.01	60.53
Graphite plate	Solid	43.3	5.4	37.9	0.5	14.4
Glass plate	Solid	121.61	30.98	90.63	4.39	54.66
Silicon wafer	Solid	138.95	3.93	135.02	5.04	0.77
Methanol[a]	Liquid	19.6	1.4	18.2	0.07	7.0

[a] Reference liquids [water, ethylene glycol, formamide, methanol] in reference [31].

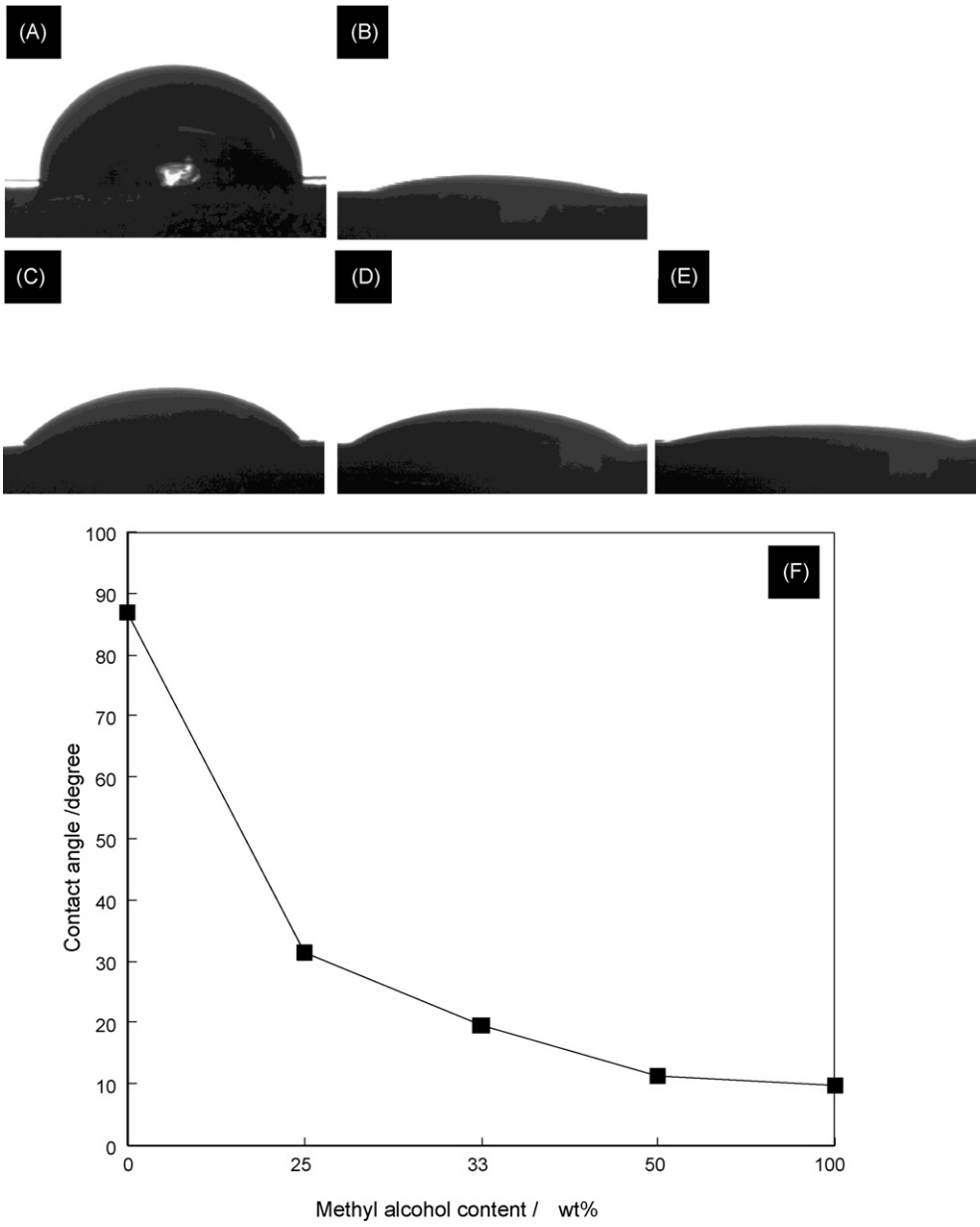

Fig. 3. Contact angle images of (A) phenolic resin, (B) methanol, mixtures at different methanol content at (C) 25 wt%, (D) 33 wt%, and (E) 50 wt%. Angles are exhibited as function of methanol content in (F).

Subsequently, the three solid substrates of glass, silicon wafer and graphite plates were used to determine the surface free-energies of the phenolic resin system under study. As a result, the measured surface free-energy of phenolic resin is 107.77, 51.63 and 56.14 mJ m^{-2} for γ_L, γ_L^{AB} and γ_L^{LW}, respectively.

As summarized in Table 1, the surface free-energy of the phenolic resin is relatively high (γ_L = 107.77 mJ m^{-2}), which would give rise to a fairly high contact angle with the graphite, which has a relatively low value at γ_S = 43.3 mJ m^{-2}. Substituting the surface energy values of phenolic resin and graphite into Eqs. (1)–(5), the contact angle between phenolic resin and graphite can be estimated as 78.9°, which compares well with the experimental value of 87.1°. This high contact angle may very well give rise to bad wetting characteristics between phenolic resin and graphite powder during mixing and thereby provide void defects at the interface that deteriorate the electrical and mechanical properties of bipolar plates.

The above observations show that it is necessary to decrease the contact angle between the graphite and the matrix material. As can be realized by rearrangement of Young's equation (see above), $\cos\theta = (\gamma_S - \gamma_{SL})/\gamma_L$, the contact angle can be decreased by decreasing the surface energy of the liquid (γ_L) and/or by decreasing the interfacial energy between the liquid and solid (γ_{SL}). One simple way to alter the surface free-energy of the resin system may be the incorporation of a secondary liquid into the resin. In this sense, it should be noticed that the surface tension of a binary mixture ($\gamma_{L,mixture}$) of two pure components ($\gamma_{L,A}$ and $\gamma_{L,B}$) can been described by the following simple linear relationship:

$$\gamma_{L,mixture} = \gamma_{L,A}\xi_A + \gamma_{L,B}\xi_B \quad (6)$$

where the coefficients ξ_A and ξ_B are bulk molar fractions, or molar fractions, of the surface area [21–23]. Accordingly, it is speculated that the surface free-energy of the matrix liquid (phenolic resin in the present study) may be decreased by adding a secondary sol-

Table 2
Comparison of contact angle values of phenolic resin, methanol and mixtures on graphite at different methanol compositions.

Methanol composition	Contact angle (degree)
0 wt% (phenolic resin)	87.1
25 wt%	31.5
33 wt%	19.6
50 wt%	11.2
100 wt% (methanol)	9.7

vent, which should necessarily be compatible with phenolic resin. For this purpose, methanol was chosen as a secondary solvent to enhance the wettability of phenolic resin with graphite because the surface free-energy of methanol is very low, viz., 19.6 mJ m^{-2}, and the contact angle with the graphite is quite low at 9.7° (see Fig. 3B).

As seen in Fig. 3 and Table 2, the contact angle of a phenolic resin and methanol mixture significantly decreases with incorporation of methanol. The contact angle of phenolic resin is 87.1° and it decreases to 31.5°, 19.6° and 11.2° for the methanol mixtures of 25, 33 and 50 wt%, respectively. From the contact angle measurement, it can be inferred that the wettability of the phenol/methanol mixture on graphite would be improved by increasing the methanol content. In addition, it should be addressed that the incorporated methanol desirably decreases the viscosity as well as the contact angle of the phenol resin, which would facilitate the mixing process of highly loaded graphite composite systems leaving a minimal void volume in the final product. Based on this finding, a 50 wt% methanol/phenolic resin mixture was used for the fabrication of bipolar plates in this study.

3.2. Electrical conductivity

For the best performance of the bipolar plates, the electrical conductivity of the different-sized graphite powders (GR75 and GR150) in the through-thickness direction was tested. Fig. 4 shows the through-thickness electrical conductivity of the graphite powder as measured while it is compressed by the universal testing machine using the experimental set-up in Fig. 1. The electrical conductivity of both GR75 and GR150 powders increases with the volume fraction of graphite during compression. Comparing these two systems, the electrical conductivity of GR75 is higher than GR150 in all the range of volume fraction, e.g., 74 and 20 S cm^{-1} at 65 wt%, respectively, which means that smaller particles give a higher electrical conductivity at the same void volume. It is thought that the smaller particles have a larger surface area than the larger particles at a fixed volume fraction and, subsequently, provide a higher degree of inter-particle contact. Since the contact points of graphite particles provide the electrical path through the particulate bed, it is concluded that the GR75 system gives higher conductivity than the GR150 system. The reverse may be true, however, when the graphite powder is mixed with the polymer resin as a composite system because the matrix polymer may be located at the interface of graphite–graphite contact points and act as an insulator to increase the contact resistance and thereby lower the electrical conductivity.

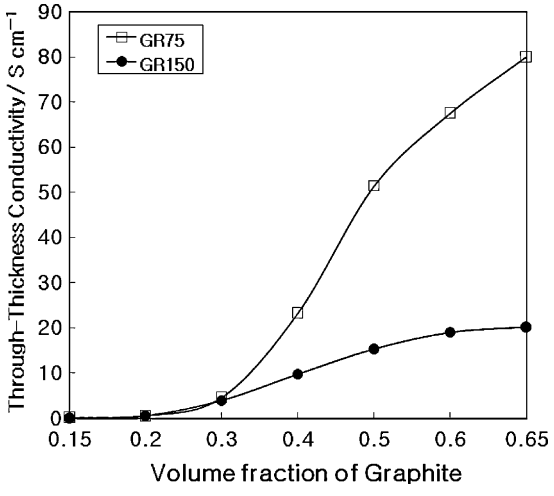

Fig. 4. Through-thickness electrical conductivity of GR75 and GR150 graphite powder plotted as function of graphite volume fraction.

For the graphite-based composite materials, the in-plane conductivity is usually about 10 times higher than that in the through-plane due to the anisotropic characteristics of graphite [24,25]. In fuel cell bipolar plates, the in-plane conductivity is more important because the bipolar plate is thin in the through-thickness direction and the area is large in the in-plane direction. Accordingly, measurements were made of the in-plane electrical conductivity of the phenolic resin–graphite composite systems each containing GR75 and GR150. In contrast with the electrical conductivity of the powders, the GR150 composite shows higher conductivity than the GR75 system over the range of graphite content. As already discussed, the smaller-particle composite system (GR75) is likely to have the larger contact points and thus the contact resistance becomes larger because the contact points are insulated with the polymer matrix.

This geometric effect of the particle size or aspect ratio may be further explained by theoretical modelling by using the models of electrical conductivity developed by Keith et al. [26], which is a modified version of the models developed by Mamunya et al. [27,28] and Clingerman et al. [29]. The model equations are as follows:

$$\log\sigma = \log\sigma_L + (\log\sigma_S - \log\sigma_L)\left(\frac{\phi-\phi_c}{F-\phi_c}\right)^k \quad (7)$$

where σ, σ_L and σ_S are the electrical conductivities (S cm^{-1}) of the composite, polymer matrix and solid filler, respectively, and the filler volume fraction (ϕ) at the percolation threshold is defined as ϕ_c. The model parameter, k, is dependent upon the filler volume fraction. The maximum filler loading (F) and the model parameters (K) are defined as

$$F = \frac{5}{(75/10 + A_s) + A_s} \quad (8)$$

$$k = \frac{K\phi_c}{(\phi-\phi_c)^{0.75}} \quad (9)$$

$$K = 0.11 + 0.03\gamma_{SL} \quad (10)$$

where A_s is the filler aspect ratio. For the model prediction, the interfacial energy (γ_{SL}) may be estimated by the Fowkes [30] equation, viz:

$$\gamma_{SL} = \gamma_L + \gamma_S - 2(\gamma_L\gamma_S)^{0.5} \quad (11)$$

where γ_L is the polymer surface energy and γ_S is the filler surface energy.

It is assumed that the composite electrical conductivity is equal to σ_L for volume fractions less than, or equal to, the percolation threshold ϕ_c. At maximum filler loading, F, the electrical conductivity is σ_S (S cm^{-1}). For the model prediction, it was decided to use the interfacial energy (γ_{SL}) between the graphite plate and phenol resin at 22.63 mJ m^{-2}, $\sigma_L = 1\times10^{-10}$ S cm^{-1}, $\sigma_S = 106.5$ S cm^{-1} and $\phi_c = 0.4$. The model prediction is compared with the experimental results in Fig. 5 for the GR75 and GR150 composite systems with $A_s = 0.1$ and 0.7, respectively. The model agrees well with the experiments and thus demonstrates that the model parameter of the

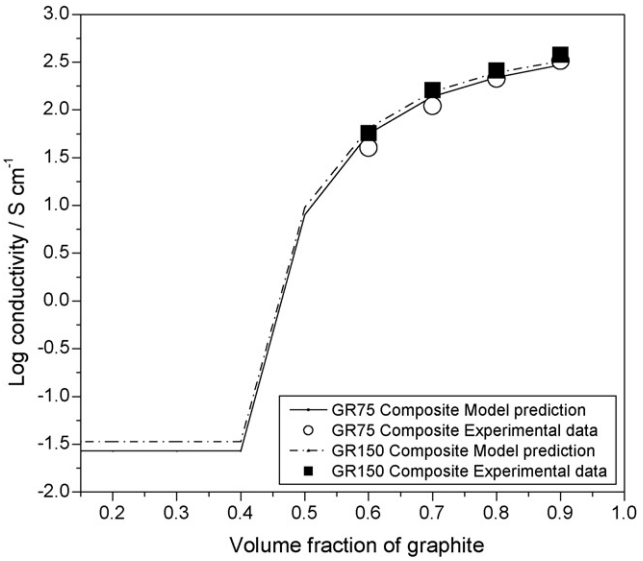

Fig. 5. Model prediction of electrical conductivity of GR75 and GR150 graphite–phenolic resin in the in-plane direction.

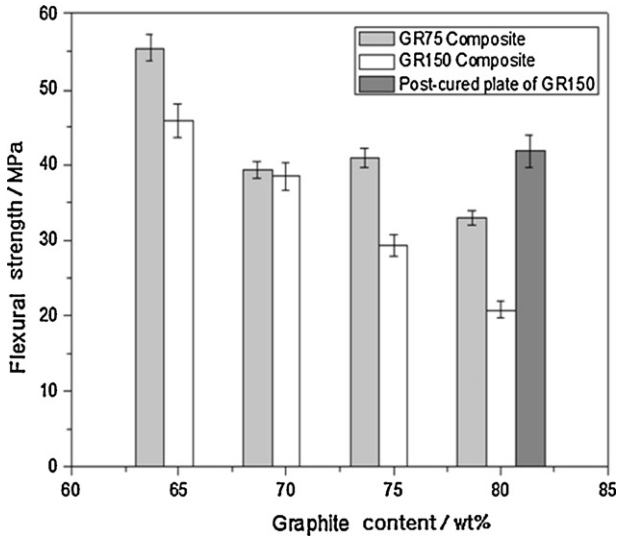

Fig. 6. Flexural strength of graphite–phenolic resin composites at different graphite contents.

geometric aspect ratio, A_s, describes well the electrical conductivity of phenolic resin–graphite composite system.

As corroborated by model prediction and experiment, the filler shape and wetting characteristics are important determinants of influencing the electrical conductivity of polymeric composites. By eliminating void defects in the composites, the electrical conductivity increases to 379 S cm^{-1}, which is one of the highest values reported for polymer-based bipolar plates at 90 wt% of graphite [31]. Although it is difficult to quantify, it should be mentioned that, in this study, the high conductivity of the composite is not achieved for specimens that include a certain level of void defects. The conductivity was not even measurable for most samples containing a substantial number of voids and this demonstrates that the electrical percolation is critically influenced by the void volume of composites. Thus it should be strongly emphasized that the processing techniques and the wetting characteristics are very important in the preparation of highly loaded composite systems, especially when the electrical properties are a major criterion for the intended application.

The in-plane and through-plane electrical conductivities of graphite composites are summarized in Table 3 for GR75 and GR150 graphite systems. As can be seen, the in-plane conductivity of composites is 5–10 times higher than the through-thickness conductivity due to the anisotropic nature of graphite structure. Furthermore, since the contact points of graphite particles provide the electrical path through the particulate graphite bed, the smaller-sized GR75 system exhibits higher electrical conductivities than the larger-sized GR150 system.

Table 3
Comparison of in-plane and through-plane electrical conductivities for graphite composites.

Graphite	Composition	In-plane conductivity (S cm^{-1})	Through-plane conductivity (S cm^{-1})
GR75	60 wt%	39.9	18.1
	70 wt%	109.7	25.9
	75 wt%	163.1	32.4
	80 wt%	212.1	39.1
GR150	60 wt%	57.0	5.0
	70 wt%	160.5	12.5
	75 wt%	237.1	29.5
	80 wt%	324.7	31.1

3.3. Mechanical properties of composite bipolar plates

The flexural strengths of composite bipolar plates containing graphite between 60 and 80 wt% are given in Fig. 6. The flexural strength of the GR75 composites is higher than that of GR150 counterparts at all loadings of graphite. The data given in Fig. 6 shows that the flexural strength of the composite bipolar plates decreases with increasing graphite content, which is found with most highly loaded composite systems because the incorporated fillers give a higher probability that cracks are initiated under the load. In addition, post-curing of the composite could increase the strength of the bipolar plates, which is indicated by the dark-grey column in Fig. 6 in the case of 80 wt% of the GR150 composite system. For this system, the flexural strength of the bipolar composite additionally post-cured at 210 °C for 10 min increases from 20.8 to 41.9 MPa. It is believed that post-curing of the composite increases the cross-linking density of the polymer chains and thereby enhances the mechanical strength.

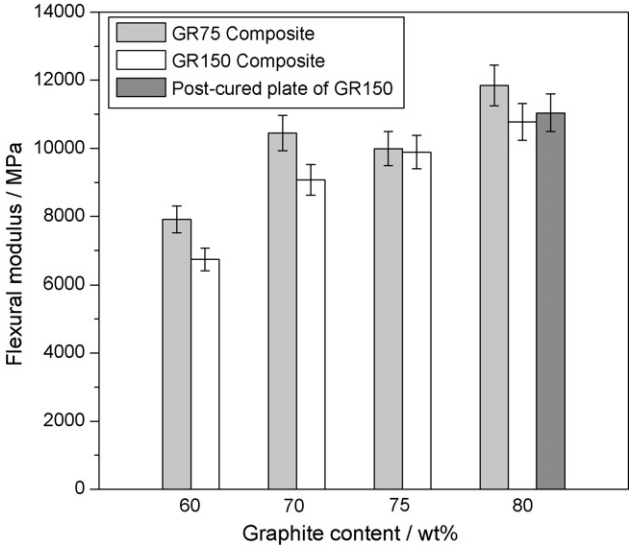

Fig. 7. Flexural modulus of graphite–phenolic resin composites at different graphite contents.

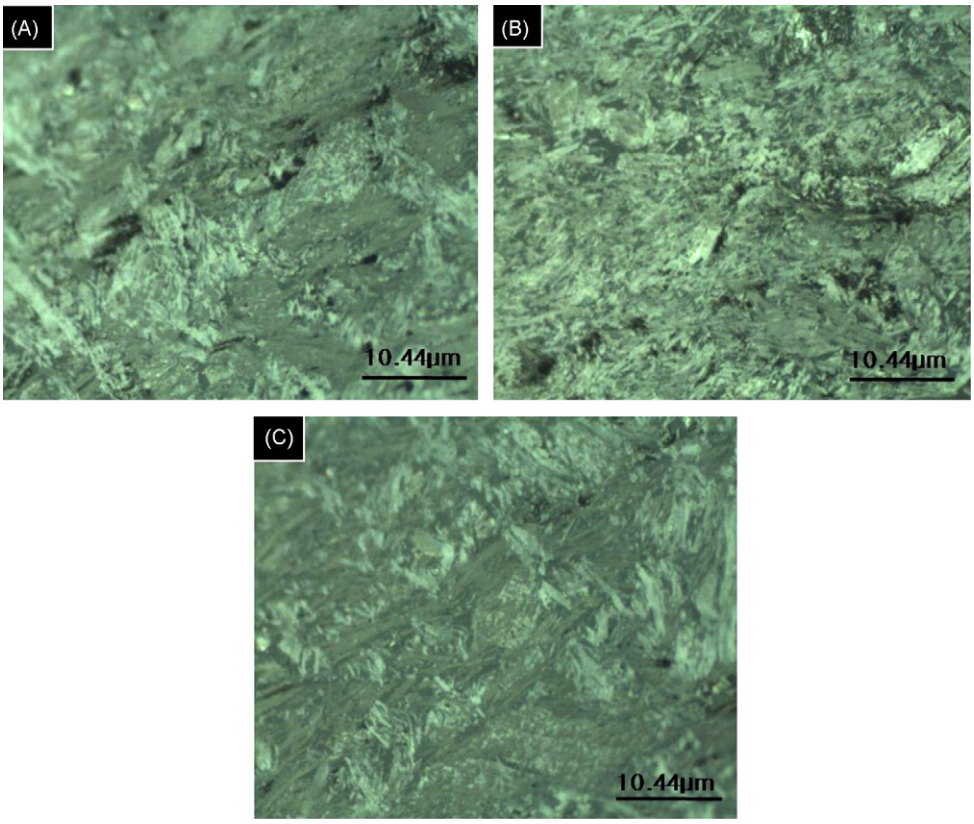

Fig. 8. Optical microscopy photographs of bipolar plate composites of (A) GR150 graphite at 65 wt%, (B) graphite GR150 at 70 wt%, and (C) graphite GR150 at 80 wt%.

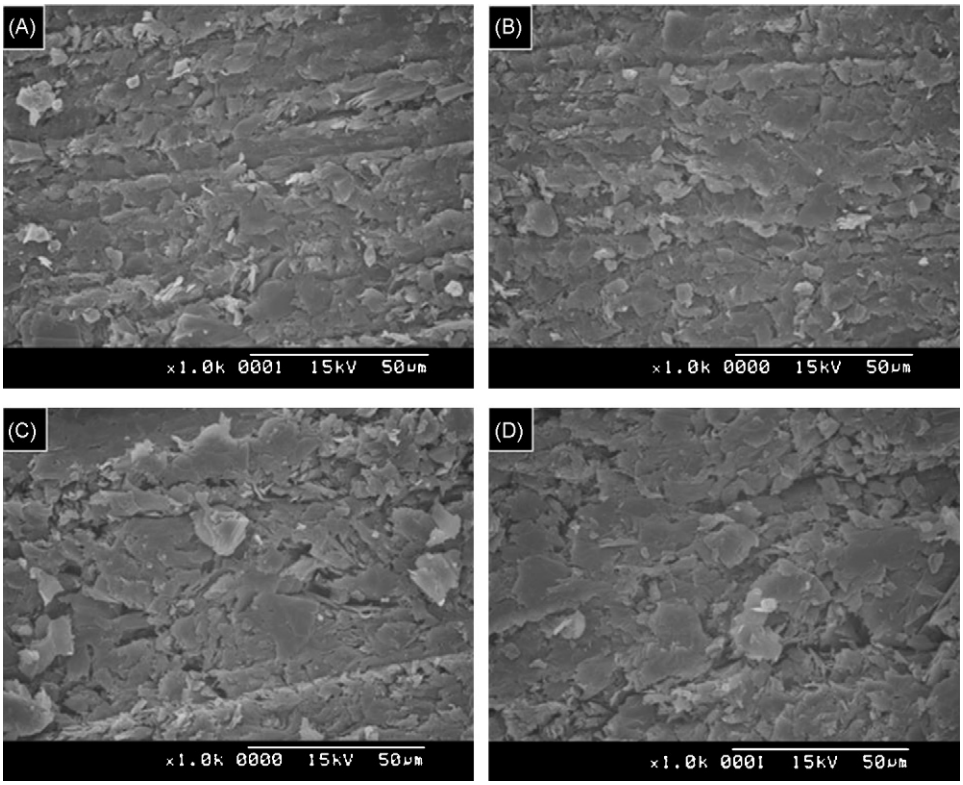

Fig. 9. Fractured surface of graphite composites at different phenolic resin contents (A) GR75 at 60 wt%, (B) GR75 at 70 wt%, (C) GR75 at 80 wt% and (D) GR150 at 80 wt%.

Table 4
Air permeability of composite bipolar plates.

Graphite	Composition	Air permeability ($cm^3\ cm^{-2}\ s$)	Conductivity ($S\ cm^{-1}$)
GR75	80 wt%	5.0×10^{-6}	212
GR150	80 wt%	7.6×10^{-6}	324
GR75	75 wt%	1.7×10^{-5}	237

The flexural modulus of composite bipolar plates with graphite loadings between 60 and 80 wt% is presented in Fig. 7. The flexural modulus of the composite bipolar plates increases with increasing graphite content, and the GR75 composite system shows higher modulus values than the GR150 system. The flexural modulus of the GR150 composite at 80 wt% is 10.7 GPa, which is raised to 11 GPa after post-curing at 210 °C for 10 min, see dark-grey column in Fig. 7.

3.4. Permeability properties of graphite composites

The air permeability values of the composite bipolar plates are given in Table 3. The air permeability of the GR150 composites ($7.6 \times 10^{-6}\ cm^3\ cm^{-2}\ s$) is higher than that of GR75 composites ($5.0 \times 10^{-6}\ cm^3\ cm^{-2}\ s$). These results indicate that the bipolar plates do not have connected pores for the gases to pass through since the permeability are within the range of the DOE permeability specification for hydrogen [32]. It is clear from the data in Table 4 that the air permeability of the composite bipolar plates decreases with increasing graphite content.

3.5. Microstructure of composite

An optical micrograph of polished cross-section of the composite is given in Fig. 8; the dark areas in the micrograph represents voids, whereas the grey and white areas are phenolic resin and graphite, respectively. It can be seen that the extent of voids at the bipolar plates decreases with increasing graphite content. When the graphite content is above 80 wt%, voids are not observed since the packing density of the graphite is high and subsequently the phenolic resin probably fills the remaining space.

Scanning election micrographs of the fractured surfaces of the bipolar plate composites (GR75 system) are shown in Fig. 9. When the graphite content is 65 wt%, the fractured surface exhibits a layered feature because the graphite plates are aligned in the in-plane direction during the compression moulding process. The layered pattern appears to decrease as the graphite content is increased, and the layered feature of the fractured surface is no longer observed for composites at 80 wt% of graphite content (Fig. 9D). It is therefore concluded that that the graphite fillers in the bipolar plates are in good contact with each other to give a well-developed electrical pathway and high electrical conductivity.

4. Conclusions

By incorporating a secondary solvent to decrease the contact angle between the matrix and graphite, a solvent-assisted graphite loading results in reduced voids to yield an excellent bipolar plate composite. The graphite content is varied between 60 and 90 wt% by adjusting the amount of methanol used in the mixing stage. The conductivity of the composite having 90 wt% graphite is as high as $379\ S\ cm^{-1}$. The flexural moduli ranges from 6.7 to 11 GPa for graphite loadings at 60 and 80 wt%, respectively. The air permeability of the composite bipolar plates decreases with the increasing graphite content.

Acknowledgments

This work was supported by the Korea Research Foundation Grant (KRF-2006-005-J04603). The author are also grateful for project and equipment support from Gyeonggi Province through the GRRC program in Sungkyunkwan University, and the WCU program (R31-2008-000-10029-0) through the Korea Science and Engineering Foundation funded by the Ministry of Education, Science and Technology.

References

[1] R. Kirchain, R. Roth, J. Power Sources 109 (2002) 71.
[2] R. Kaiser, H.G. Fritz, C.D. Eisenbach (Eds.), Proceedings of the 18th Stuttgarter Kunststoffkolloquium, Sprint Druck, Stuttgart, 2003, pp. 3–4.
[3] D. Busick, M. Wilson, D.H. Doughty, L.F. Nazar, M. Arakawa, H. Brack, K. Naoi (Eds.), New Materials for Batteries and Fuel Cells, Materials Research Society Symposium, Pennsylvania, 2000, pp. 247–251.
[4] B.K. Kakati, D. Deka, Energy Fuels 21 (2007) 1681–1687.
[5] J. Wind, A. LaCroix, S. Braeuninger, P. Hedrich, C. Heller, M. Schudy, in: W. Vielstich, H.A. Gasteiger, A. Lamm (Eds.), Technology and Applications, vol. 3, Wiley & Sons, New York, 2003, pp. 294–307.
[6] J. Huang, D.G. Baird, J.E. McGrath, J. Power Sources 150 (2005) 110–119.
[7] G. Hoogers, Fuel Cell Technology Handbook, CRC Press, Boca Raton, 2003, pp. 4-21–4-23.
[8] M.H. Oh, Y.S. Yoon, S.G. Park, Electrochim. Acta 50 (2004) 777–780.
[9] E.A. Cho, U.S. Jeon, H.Y. Ha, S.A. Hong, I.H. Oh, J. Power Sources 125 (2004) 178–182.
[10] M. Wu, L.L. Shaw, Int. J. Hydrogen Energy 30 (2005) 373–380.
[11] A. Hermann, T. Chaudhuri, P. Spagnol, Int. J. Hydrogen Energy 30 (2005) 1297–1302.
[12] M. Wu, L. Shaw, J. Power Sources 136 (2004) 37–44.
[13] A. Knop, L. Pilato, Chemistry and Application of Phenolic Resins, Springer-Verlag, Berlin, 1979, p. 28.
[14] Y.K. Lee, D.J. Kim, H.J. Hwang, M. Rafailovich, J. Appl. Polym. Sci. 89 (2003) 2589.
[15] E. Middelman, W. Kout, B. Vogelaar, J. Power Sources 118 (2003) 44–46.
[16] A. Heinzel, F. Mahlendorf, O. Niemzig, C. Kreuz, J. Power Sources 131 (2004) 35–40.
[17] A. Müller, P. Kauranen, A. von Ganski, B. Hell, J. Power Sources 154 (2006) 467–471.
[18] B.D. Cunningham, J. Huang, D.G. Baird, J. Power Sources 165 (2007) 764–773.
[19] F.M. Fowkes, in: K.L. Kittal (Ed.), Physicochemical Aspects of Polymer Surfaces, Plenum Press, New York, 1983, pp. 583–603.
[20] C.J. Van Oss, R.J. Good, M.K. Chaundhury, Langmuir 4 (1998) 884–891.
[21] K.A. Connors, J.L. Wright, Ann. Chem. 61 (1989) 194–198.
[22] Á. Piñeiro, P. Brocos, R. Bravo, A. Amigo, Fluid Phase Equilib. 182 (2001) 337–352.
[23] K. Kirmse, H. Morgner, Langmuir 22 (2006) 2193–2199.
[24] B. Cunningham, D.G. Baird, J. Mater. Chem. 16 (2006) 4358–4388.
[25] B. Cunningham, D.G. Baird, J. Power Sources 168 (2007) 418–425.
[26] J.M. Keith, J.A. King, R.L. Barton, J. Appl. Polym. Sci. 102 (2006) 3293.
[27] E.P. Mamunya, V.F. Shumskii, E.V. Lebedev, Polym. Sci. 36 (1994) 835.
[28] E.P. Mamunya, V.V. Davidenko, E.V. Lebedev, Compos. Interface 4 (1997) 169.
[29] M.L. Clingerman, E.H. Weber, J.A. King, K.H. Schulz, J. Appl. Polym. Sci. 88 (2003) 2280.
[30] F.M. Fowkes, Ind. Eng. Chem. 56 (1964) 40.
[31] R. Holm, Electric Contacts, Theory and Applications, 4th ed., Springer-Verlag, Berlin, 1967.
[32] K. Robberg, V. Trapp, in: W. Vielstich, H.A. Gasteiger, A. Lamm (Eds.), Technology and Applications, vol. 3, Wiley & Sons, New York, 2003, pp. 308–314.